

RESEARCH ARTICLE

Imaging mass spectrometry identifies prognostic ganglioside species in rodent intracranial transplants of glioma and medulloblastoma

Leonardo Ermini¹, Elena Morganti¹, Alexander Post¹, Behzad Yeganeh¹, Isabella Caniggia^{2,3,4}, Michael Leadley¹, Claudia C. Faria^{5,6}, James T. Rutka⁵, Martin Post^{1,3,4*}

1 Program in Physiology and Experimental Medicine, Peter Gilgan Centre for Research and Learning, Hospital for Sick Children, Toronto, Ontario, Canada, **2** The Lunenfeld-Tanenbaum Research Institute, Mount Sinai Hospital, Toronto, Ontario, Canada, **3** Institute of Medical Science, University of Toronto, Ontario, Canada, **4** Department of Physiology, University of Toronto, Ontario, Canada, **5** Division of Neurosurgery, Arthur and Sonia Labatt Brain Tumour Research Centre, Hospital for Sick Children, Toronto, Ontario, Canada, **6** Instituto de Medicina Molecular, Faculdade de Medicina, Universidade de Lisboa, Lisbon, Portugal

* martin.post@sickkids.ca



OPEN ACCESS

Citation: Ermini L, Morganti E, Post A, Yeganeh B, Caniggia I, Leadley M, et al. (2017) Imaging mass spectrometry identifies prognostic ganglioside species in rodent intracranial transplants of glioma and medulloblastoma. *PLoS ONE* 12(5): e0176254. <https://doi.org/10.1371/journal.pone.0176254>

Editor: Akos Vertes, George Washington University, UNITED STATES

Received: May 26, 2016

Accepted: April 8, 2017

Published: May 2, 2017

Copyright: © 2017 Ermini et al. This is an open access article distributed under the terms of the [Creative Commons Attribution License](https://creativecommons.org/licenses/by/4.0/), which permits unrestricted use, distribution, and reproduction in any medium, provided the original author and source are credited.

Data Availability Statement: All relevant data are within the paper and its Supporting Information files.

Funding: This work was supported by operating grants (FND-143309 to MP; MOP-14096 to IC) from the Canadian Institutes of Health Research (CIHR) and an infrastructure grant from the Canadian Foundation for Innovation (12156 to MP). The funders had no role in study design, data collection and analysis, decision to publish, or preparation of the manuscript.

Abstract

Matrix-assisted laser desorption ionization (MALDI) imaging mass spectrometry (MALDI-MSI) allows us to investigate the distribution of lipid molecules within tissues. We used MALDI-MSI to identify prognostic gangliosides in tissue sections of rat intracranial allografts of rat glioma and mouse intracranial xenografts of human medulloblastoma. In the healthy adult rodent brain, GM1 and GD1 were the main types of glycolipids. Both gangliosides were absent in both intracranial transplants. The ganglioside GM3 was not present in the healthy adult brain but was highly expressed in rat glioma allografts. In combination with tandem mass spectrometry GM3 (d18:1/C24:0) was identified as the most abundant ganglioside species in the glioma allotransplant. By contrast, mouse xenografts of human medulloblastoma were characterized by prominent expression of the ganglioside GM2 (d18:0/C18:0). Together, these data demonstrate that tissue-based MALDI-MSI of gangliosides is able to discriminate between different brain tumors and may be a useful clinical tool for their classification and grading.

Introduction

Gangliosides are glycolipids containing ceramide and sialic oligosaccharides (named also glycosphingolipids). They are situated in the external leaflet of the cell membrane and are copiously expressed in the central nervous system. In tumor cells the rate of uptake and/or shedding of gangliosides in the microenvironment surrounding the cellular membrane is greatly increased [1]. GM3 and GD3 are the major gangliosides in embryonic brains. The expression of these simple gangliosides decreases with advancing brain development while that of

Competing interests: The authors have declared that no competing interests exist.

complex gangliosides (GM1, GD1, and GT1) increases [2]. Similar to the embryonic brain, simple gangliosides (GM3 and GD3) are the most common gangliosides present on the cell surface in neoplastic tissues. In human gliomas, gangliosides have an altered conformation and concentration matched to normal grey and white matter of brain. The major gangliosides GM1, GD1a, and GT1b are markedly reduced in gliomas while gangliosides GM3 and GD3 prevail [3]. In human medulloblastoma, the most common malignant pediatric brain tumor, the main gangliosides, based on glycosphingolipid analysis of a medulloblastoma cell line, are GM2, GM3, and GD1a [4, 5]. In neoplastic tissues, the biological functions of gangliosides are influenced by changes of their structure [6, 7]. For example, in neuroblastoma, the short ganglioside GD2 containing the ceramide 16:0 has more immunosuppressive activity than GD2 gangliosides comprising longer ceramide chains (24:0 or 24:1), which are more abundant in non-pathological tissue [8]. These changes in ganglioside expression in tumours have led to their use as diagnostic and prognostic molecular markers for certain neural tumours [9–12]. However, classification, grading and prognosis of human brain tumours based on histological features of ganglioside expression have been limited by the lack of a method to visualize distinct ganglioside species. MALDI imaging mass spectrometry (MALDI-MSI) is a powerful technique to visualize the distribution of several type of molecules within tissues [13]. MALDI-MSI has extensively been used to visualize various lipids in tissues [14–21]. Cryosections are coated with a specific MALDI matrix and subsequently subjected to ionization thanks to a laser beam that moves across the tissue surface. Analyte ions are desorbed from the tissue sections and successive mass spectra are detected. The molecular distribution of the analytes as well as their intensity is then obtained as function of spatial coordinates. Several reports have shown the suitability of MALDI-MSI for analysis of ganglioside molecular species in brain tissues [20, 22–25], but this MSI technique has to our knowledge not been applied to brain tumors. Here we first investigated ganglioside metabolism and distribution in rat intracranial allografts of rat glioma using MALDI-MSI. The identity of discovered gangliosides was confirmed by LC-MS/MS analysis. To verify that MALDI-MSI of gangliosides could discriminate between different brain cancers we also analysed mouse intracranial xenografts of human medulloblastoma.

Material and methods

Cell lines and animals

Rat 9L gliosarcoma cell line [26] was generously donated by Dr. Roberto Diaz, Hospital for Sick Children, Toronto, Canada. The human medulloblastoma Daoy cell line [4] was kindly provided by Dr. Annie Huang, Hospital for Sick Children, Toronto, Canada. Athymic nude mice and Wistar rats were obtained from the Charles River Laboratories (Saint-Constant, QC).

Tissue transplants

Animal studies were approved by the Institutional Animal Care Committee of the University of Toronto and the Hospital for Sick Children (Toronto, Canada) and performed according to their policies and regulations. The glioma and medulloblastoma cell lines were injected into the brain of Wistar rats or athymic nude mice using a stereotactic frame. Animals were operated under isoflurane anesthesia (3–4% in 1L O₂ for induction and 1–2% in 1L O₂ for maintenance) while meloxicam (5mg/Kg, subcutaneous) was given as analgesic. All animals received meloxicam (5mg/Kg, subcutaneous) once daily for 48h after surgery to avoid any pain. Rodents were monitored daily for clinical signs of tumour growth, including hunched or abnormal posture, lack of grooming, weight loss exceeding 20% of body weight, anorexia, or abnormal

ambulation. The presence of any of these findings was considered an endpoint and mice were euthanized using a CO₂ chamber.

MALDI-mass spectral imaging

Preparation of brain tissue sections. The quick frozen brain tissue block was mounted onto the specimen disc of a cryostat (Leica Microsystems, Richmond Hill, ON) using optimal cutting temperature (OCT) compound (Sakura Finetek, Torrance, CA). The brain sections were horizontally sliced at a thickness of 12 μm at -15°C and mounted onto indium tin oxide (ITO)-coated glass slides. A thin matrix layer was applied to the brain sections using an automated MALDI plate matrix deposition system (TM-Sprayer™, Leap Technologies, Carrboro, NC). A total of 5 mL of 9-aminoacridine (15 mg/mL in methanol; Sigma-Aldrich, St. Louis, MO) was sprayed per slide during 4 passes at 80°C with a velocity of 400 mm/min and a line spacing of 3 mm.

MALDI imaging mass spectrometry. The acquisition of the images was performed as previously described [17, 27, 28]. A time-of-flight tandem mass spectrometer (SCIEX TOF/TOFTM 5800 System; SCIEX, Vaughan, ON) was used to acquire the images. MALDI mass spectra were obtained using a Nd:YAG laser (349 nm) at 3 ns pulse width and 400 Hz firing rate. To install the ITO-coated glass slides in the ionization chamber, we used a special holder (SCIEX) having concavities. The data were acquired in the negative-ion reflector mode using an external calibration method. The external calibration gangliosides (Avanti Polar Lipids, Alabaster, AL; Sigma-Aldrich, St Louis, MO) were deposited on the ITO-coated slides to minimize mass shift (see S1 Fig). A total of 200 laser shots per point were irradiated (1 s/point) and the interval between data points are 75 μm . The mass spectrometric data were processed using a specialized script of Analyst software (SCIEX) at a mass resolution of 0.1 amu and images were visualized using TissueView software (SCIEX). The imaging experiments were repeated with 3 different intracranial transplanted mice and rat brains. The gangliosides identified by MALDI-MSI are listed in S1 Table.

Immunohistochemistry

Cryostat sections of 10- μm thickness were cut from mouse and rat brains and stained for Cholera Toxin B (CTB) and Neuropilin-1 (NRP-1) as described previously [29]. Briefly, tissue sections were rehydrated and blocked for one hour at room temperature followed by incubation with either the biotin-conjugated CTB subunit (1:500; Sigma, St Louis, MO) or rabbit anti-NRP1 (1:1000; gift of Dr. D.D. Ginty, Harvard University) antibody overnight at 4°C in a humidified chamber. The primary antibody was detected by using a biotinylated secondary anti-rabbit IgG (Jackson ImmunoResearch Laboratories). The biotin complexes were visualized using an ABC kit (Vector laboratories, Burlington, ON). As a negative control, sections were processed as above but CTB subunit or primary antibody was omitted.

Rat brain glycosphingolipid extraction

Tissue sections were sliced at a thickness of 80 μm at -15°C in cryostat and mounted onto superfrost microscope slides (Fisher Scientific, Ottawa, ON). Squares of 2 mm of the pathological and physiological brain area were cut out, weighed, transferred to siliconized screw capped glass extraction tubes and homogenized using a Polytron tissue grinder (three 10-s bursts with 20-s intervals) in 4 volumes (4 ml/g wet weight) water. To the homogenate were then added 2.67 volumes (based on the total aqueous volume) of ambient temperature (RT) methanol and 1.33 volumes of chloroform, tubes capped and mixed vigorously. The mixture was centrifuged at 450 x g at RT for 15 min and the supernatant was transferred to a fresh screw-capped tube.

A small (0.173) volume of water was added and the mix was centrifuged again at 450 x g at RT for 15 min. The supernatant was then loaded on C18 Sep-Pak. The column was washed with 3 ml each of the following: (i) chloroform-methanol-water (2:43:55) and (ii) methanol-water (1:1). The gangliosides were eluted with 3 ml of methanol, collected into a fresh screw capped tube and evaporated to dryness under a stream of dry nitrogen at 45 °C. The gangliosides were then re-dissolved in 2.5 volumes of methanol, based on the original tissue weight adjusting for recovery of “recovered extract volume” and subjected to LC-MS/MS analysis.

LC-MS/MS analysis

LC-MS/MS was performed on an Agilent 1200 HPLC (Agilent Technologies: Santa Clara, California, USA) and a Sciex API4000 Mass Spectrometer (Sciex, Vaughan, ON). Chromatography ran at a flow rate of 500 μ L/min on an Agilent SB-Phenyl 3.5 μ , 3.0x50 mm column. The mobile phase consisted of A = Water and B = 10/45/45 Water/Methanol/Acetonitrile, both A and B containing 10 mM Ammonium Acetate. The mass spectrometer was operated in negative ESI mode with a source temperature of 600°C, an ESI voltage of -4,500, DP of -40, and EP of -10 volts. Data was acquired in by single MS with Q1 scanning from 1,100 m/z to 1,600 m/z. LC/MS/MS precursor ion scanning of 290 m/z Q3 and 1,200 m/z to 1,400 m/z Q1 was performed with the same MS parameters as above and additional settings of -50 CE (N_2 gas) and -15 CXP volts. Data handling was performed using Sciex Analyst 1.6 software.

Results

We first investigated the expression and distribution of GM1 and GD1 in brains of naïve adult Wistar rat using MALDI-MSI. The GM1 (d18:1/C18:0; m/z 1545; M-H) and (d20:1/C18:0; m/z 1573; M-H) gangliosides were present throughout the cerebral cortex (Fig 1). Expression of GD1 (d18:1/C18:0; m/z 1874; [M+Na-2H] and d20:1/c18:0; m/z 1886; [M+Na-2H]) gangliosides in the cortex overlapped with that of the GM1 (d18:1/C18:0) ganglioside. Analysis of our GD1 standards confirmed that GD1 gangliosides can lose their sialic acid moiety in the negative reflectron ion mode during MALDI-MSI [22] and that the resulting GD1 derivatives ionize at the same mass as GM1 (see S2 Fig). The distribution of GM1 in the brain was also identified by staining with the B subunit of cholera toxin (Fig 2B), which binds to GM1 [30]. The CTB staining revealed that GM1 was present in the subcortical white matter and less pronounced in the cortex. Thus, it is plausible that the MALDI-MSI detection of GM1 in the cortex is partially due to GD1 fragmentation. Also, the GD1 gangliosides are particularly abundant in the cortex. Therefore, we have labelled the peaks at 1545 and 1573 m/z as GM1/GD1-sialic acid (GM1/GD1-sa). Moreover, changing the scale and intensity of the ions revealed that GM1 also localized to the white matter (see S3 Fig).

The localization of the GM1 and GD1 gangliosides was not altered in the areas of rat brains containing an intracranial allograft of glioma (Fig 2A). However, both types of ganglioside were absent in the tumor (Fig 2A, circle). Negative CTB staining of the rat glioma (Fig 2B) corroborated our GM1 findings using MALDI-MSI (Fig 2A). The glioma cells were positively identified by neuropilin-1 (NRP-1) immunohistochemistry (Fig 2B). NRP-1 is a cell surface glycoprotein that is highly expressed in many cancers, including glioma [31] and medulloblastoma [32].

The control rat brains and intracranial allografts of rat glioma were also analysed for the presence of GM2 and GM3. While the GM2 (d18:0/c18:0; m/z 1385; [M-H]) ganglioside was not detected in the control and allograft brain sections (S4 Fig), GM3 with a d18:1/C24:0 ceramide (m/z 1264; M-H) exclusively localized to the glioma transplant area (Fig 3A). Specifically, merging MALDI-MSI and H&E strongly demonstrated the unique expression of GM3

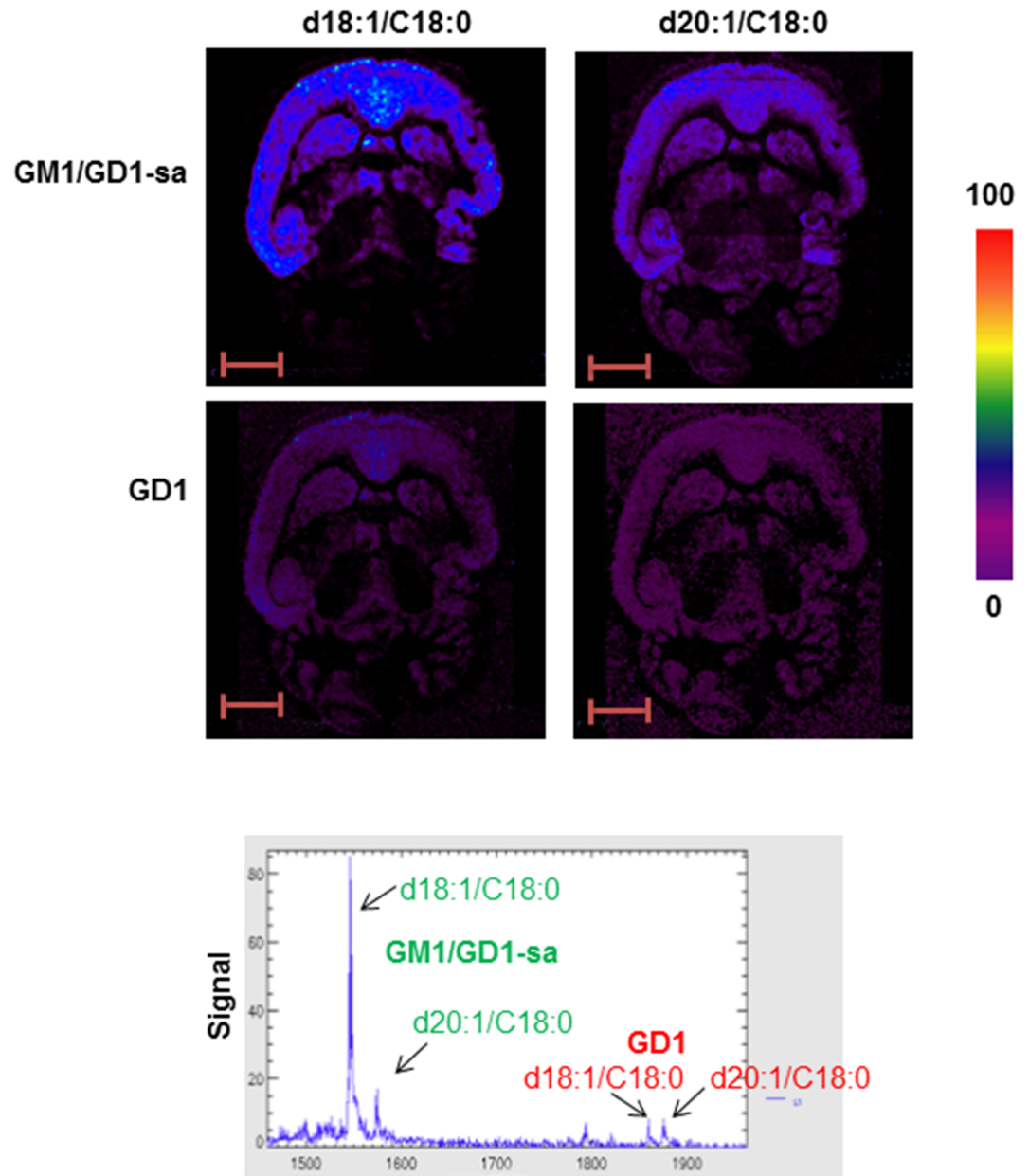


Fig 1. MALD-MSI of GM1 and GD1 in adult rat brain. MSI and mass spectra of GM1/GD1-sialic acid (H-) d18:1 (m/z 1545) and 20:1 (m/z 1573), GD1 ([M-H]²⁻) d18:1 (m/z 1874) and 20:1 (m/z 1886) in healthy adult Wistar rat brain. Intensities of the ions are represented in color based on the intensity scale provided. Arrows indicate the peaks visualized in MSI. GD1-sa = GD1-sialic acid.

<https://doi.org/10.1371/journal.pone.0176254.g001>

(d18:1/C24:0) in the glioma allotransplant (Fig 3B). In addition, merging MALDI-MSI with H&E highlighted the absence of GM1 gangliosides from the glioma allograft (Fig 3B).

We confirmed the MALDI-MSI data by LC-MS/MS analysis. The glioma allograft and a comparable non-pathological area were excised from 80- μ m thick brain cryosections (S5A Fig) and subjected to glycosphingolipid extraction and detection by tandem mass spectrometry. The LC-MS/MS analysis verified the change in distribution from GM1 towards GM3 gangliosides in the glioma allograft compared to non-pathological brain tissue (S5B and S5C Fig).

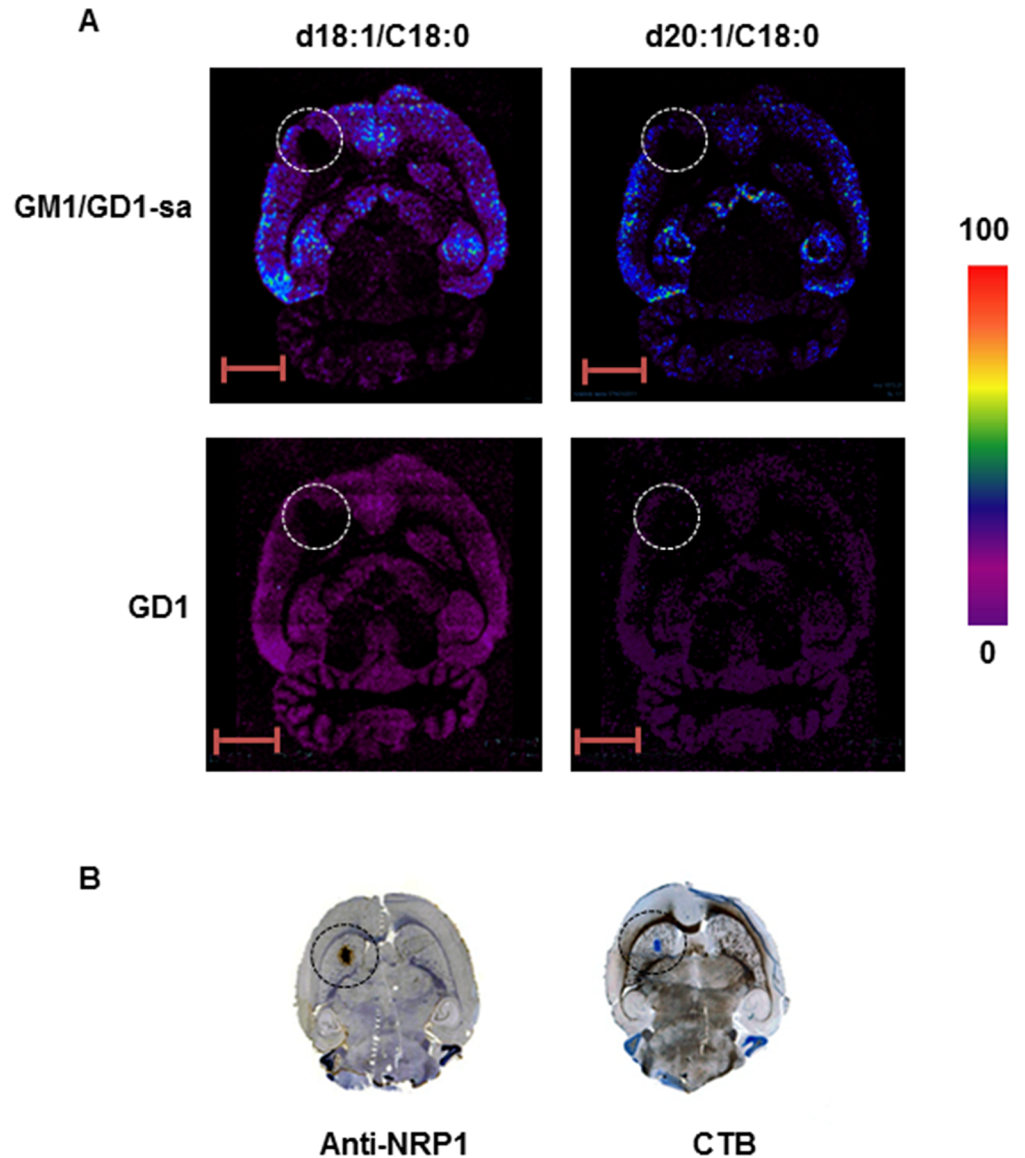


Fig 2. MALD-MSI of GM1 and GD1 in intracranial allografts of rat glioma. (A) MSI of GM1/GD1-sialic acid (H-) d18:1 (m/z 1545) and 20:1 (m/z 1573), GD1 [M+Na-2H] d18:1 (m/z 1874) and 20:1 (m/z 1886). Intensities of the ions are represented in color based on the intensity scale provided. (B) Distribution of GM1 and NRP-1 by immunostaining with CTB and anti-NRP1 antibodies, respectively, in intracranial allografts of rat glioma. Circles indicate the position of the xenograft. Scale bar: 5 mm. GD1-sa = GD1-sialic acid.

<https://doi.org/10.1371/journal.pone.0176254.g002>

The most representative GM3 species in the glioma was GM3 (d18:1/C24:0; m/z 1264). Precursor ion scanning for m/z 290 fragment in negative mode confirmed the ganglioside identity of this mass peak. Moreover, mass spectral comparison between GM1/GM3 standards and glioma glycosphingolipid extract validated that the GM3 species in the cancer contained the ceramide d18:1/C24:0 (S5D Fig).

We then analyzed intracranial mouse xenografts of human medulloblastoma using the same approach. We initially examined the expression and distribution of GM1 and GD1 in the naïve adult mouse brain and found that the distribution of these two gangliosides (Fig 4) matched that of the rat brain (Fig 1). The distribution of these two ganglioside species was

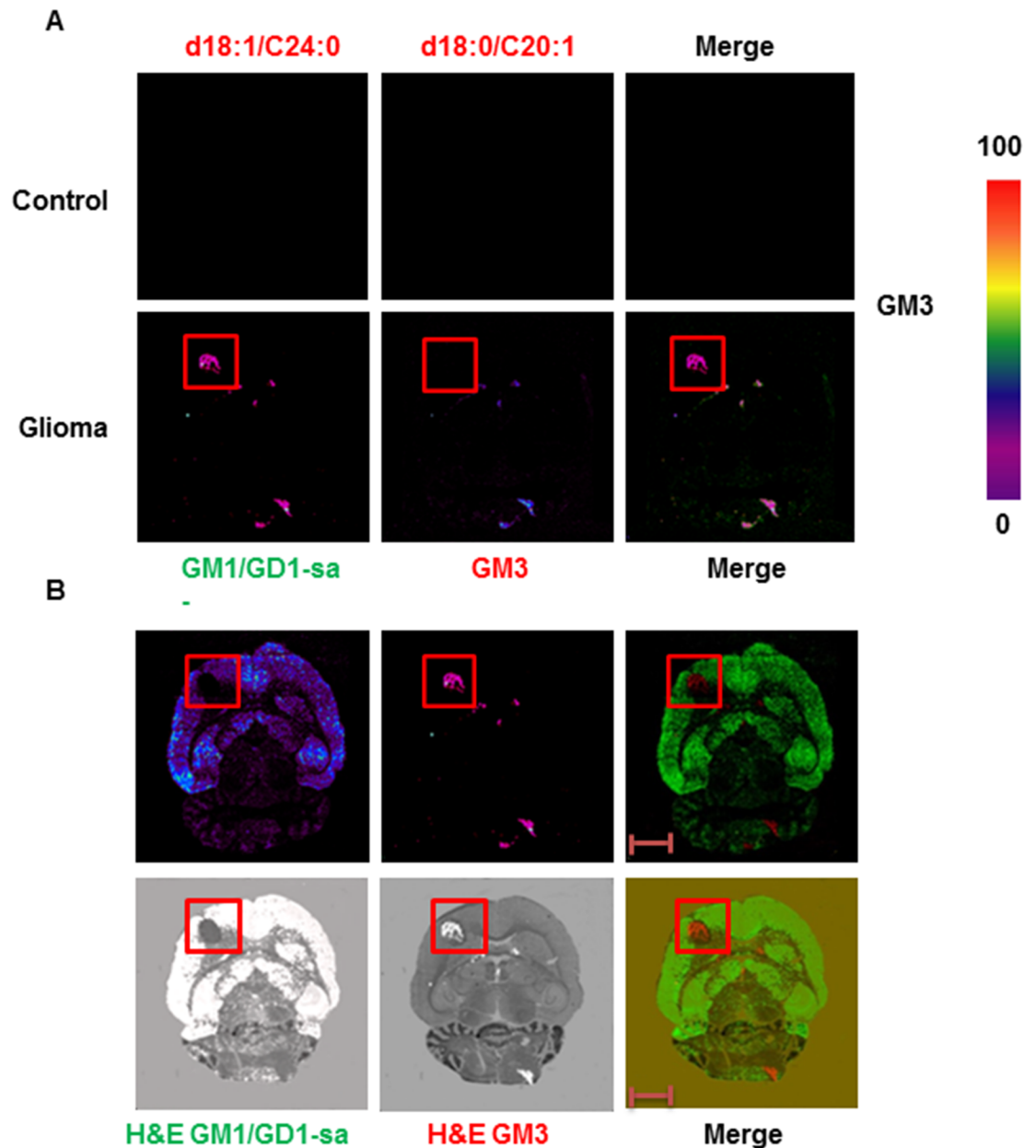


Fig 3. MALDI-MSI of GM3 in intracranial allografts of rat glioma. (A) MSI of GM3 (H-) d18:1 24:0 (m/z 1264) and d18:0 20:1 (m/z 1208) in intracranial allografts of rat glioma. Intensities of the ions are represented in color based on the intensity scale provided. (B) Molecular histology distribution of GM1/GD1-sialic acid (d18:1/C18:0) and GM3 (d18:1/C24:0) in intracranial allografts of rat glioma. Red squares indicate the position of the glioma xenograft. Scale bar: 5 mm. GD1-sa = GD1-sialic acid.

<https://doi.org/10.1371/journal.pone.0176254.g003>

maintained in the mouse brains with the intracranial xenografts of human medulloblastoma (Fig 5A). The intracranial xenografts of human medulloblastoma were then examined by MALDI-MSI for the presence of GM2 and GM3. By contrast to glioma allografts, ganglioside GM3 (d18:1/C24:0) was not detected in the medulloblastoma xenograft (Fig 5A). Only the internal standard (IS) was visible. However, MALDI-MSI revealed a GM2 species with a d18:0/C18:0 ceramide (m/z 1385; M-H) that exclusively localized to the medulloblastoma xenograft area (Fig 5A and 5B). Merging of MALDI-MSI and H&E confirmed the expression

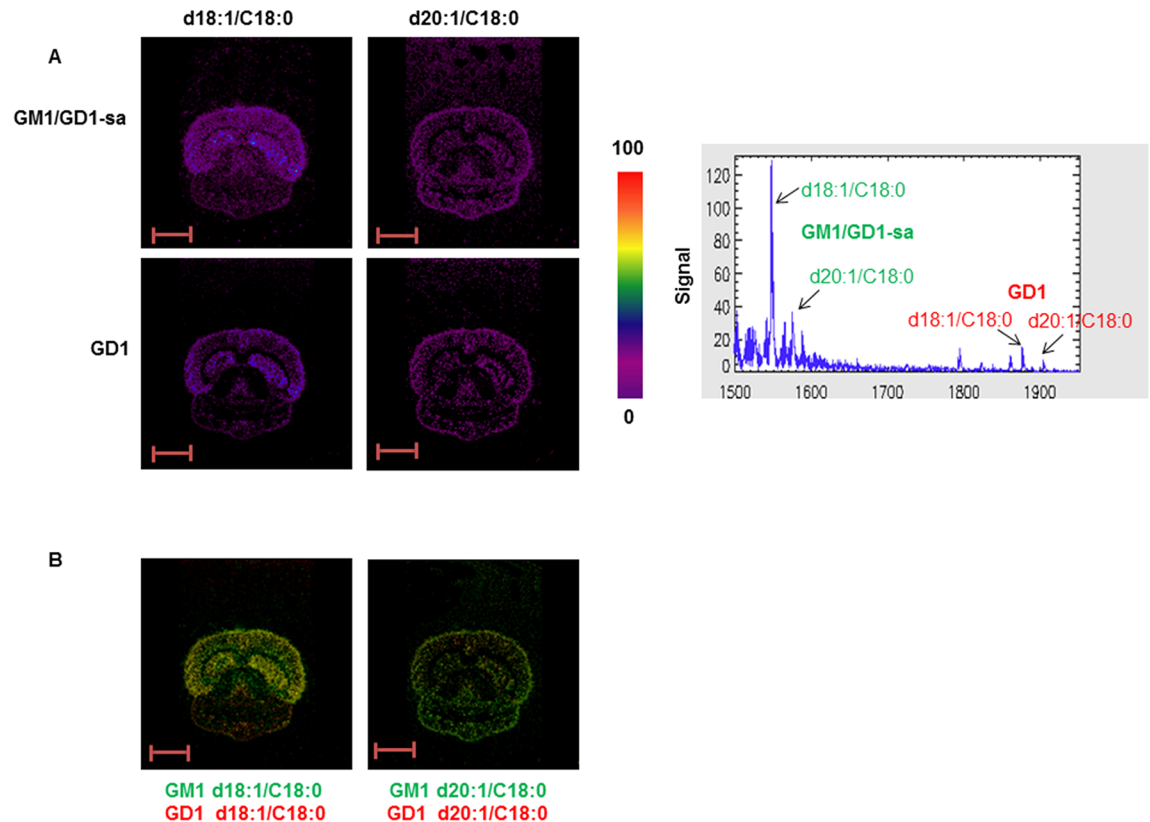


Fig 4. MALDI-MSI of GM1 and GD1 in adult mouse brain. (A) MSI and mass spectra of GM1/GD1-sialic acid (H⁻) d18:1 (m/z 1545) and 20:1 (m/z 1573), GD1 [M+Na-2H] d18:1 (m/z 1874) and 20:1 [M+K-2H] (m/z 1902). Intensities of the ions are represented in color based on the intensity scale provided. Arrows indicate the peaks visualized in MSI. (B) Overlap of the distribution of GM1/GD1-sialic acid and GD1 species in healthy adult mouse brain. Scale bar: 4 mm. GD1-sa = GD1-sialic acid.

<https://doi.org/10.1371/journal.pone.0176254.g004>

of GM2 (d18:0/C18:0) in the medulloblastoma xenograft (Fig 5D). The medulloblastoma cells were positively identified by NRP-1 immunohistochemistry (Fig 5C).

Discussion

Here we show the expression and distribution of various types of ganglioside in normal adult rodent brains and in intracranial allo- and xenografts of rat glioma and human medulloblastoma, respectively, using MALDI-MSI. In line with previous reports, the major gangliosides within the normal rodent brain are GM1 and GD1 [2]. GD1 can lose its sialic acid moiety in the negative reflectron ion mode during MALDI-MSI and, in that instance, it will be detected as a GM1 species [22]. The observed similar distribution of GM1 and GD1 gangliosides in the rat and mouse brain and the white matter staining of GM1 with CTB supports the idea that the GM1 signals in the cortex is partially derived from GD1 gangliosides.

Abnormal ganglioside expression in brain cancer and the roles of these glycosphingolipid in brain tumor development, progression, and treatment have been reported in several studies [33, 34]. By MALDI-MSI we identified GM3 as the predominant ganglioside species in the rat glioma allograft. GM3 is the simplest ganglioside oligosaccharide and serves as a precursor for most of the more complex ganglioside species including GD3, GM2 and GD2 [35]. GM3 is strongly expressed in the human cerebellum between 21 and 25 weeks of gestation, a period of intense cell proliferation. At 27 weeks, there is a significant reduction in its expression and

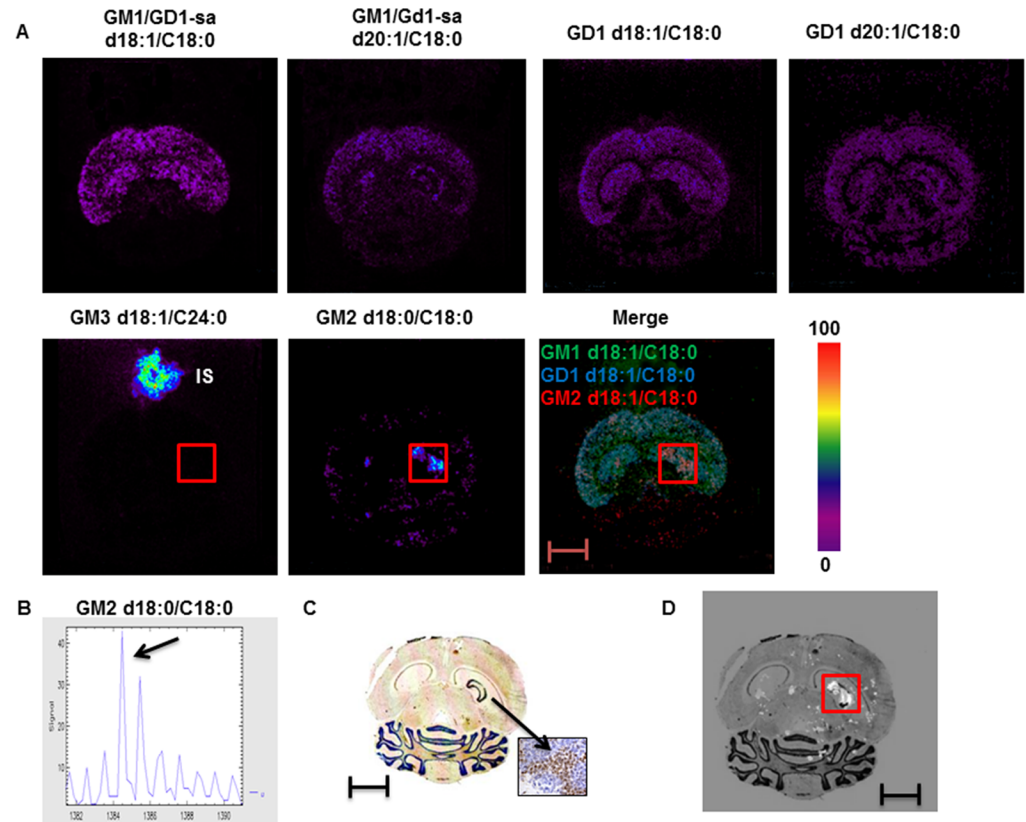


Fig 5. MALDI-MSI of gangliosides in intracranial xenografts of human medulloblastoma. (A) MSI of GM1/GD1-sialic acid (H-) d18:1 (m/z 1545) and 20:1 (m/z 1573), GD1 ([M-H]²⁻) d18:1 (m/z 1874) and 20:1 (m/z 1902), GM3 (H-) d18:1 c24:0 (m/z 1264) and GM2 (H-) d18:0 c18:0 (m/z 1385) in intracranial xenografts of human medulloblastoma. Intensities of the ions are represented in color based on the intensity scale provided. (B) Mass spectra of GM2 (d18:0/C18:0) in intracranial xenografts of human medulloblastoma. (C) Distribution of Neuropilin-1 by immunostaining with anti-NRP1 antibodies in intracranial xenografts of human medulloblastoma. The insert is a magnification 40 x of the glioma area. (D) Molecular histology distribution of GM2 (d18:0/C18:0) in intracranial xenografts of human medulloblastoma. Squares indicate the position of the medulloblastoma graft. Scale bar: 4 mm. GD1-sa = GD1-sialic acid.

<https://doi.org/10.1371/journal.pone.0176254.g005>

GM3 is virtually absent in the brain by the second postnatal month [36]. In contrast, GM3 is overexpressed in neoplastic tissues and is the most common type of ganglioside present in tumor cells [37]. The role of GM3 has mostly been studied in the apoptosis and drug resistance of neoplastic cells [38–41]. Whether the GM3 (d18:1/C24:0) species plays a role in these processes is unknown as in previous studies the chemical structure of GM3 was not determined [42].

The ganglioside profile in brain tumors has been shown to correlate with tumor histopathological origin, malignancy grade, invasiveness, and progression [43]. In the present study, we found that MALDI-MSI screening for gangliosides was able to distinguish between two types of brain cancer. MALDI-MSI identified a medulloblastoma xenograft by expression of the ganglioside GM2 while glioma allografts expressed GM3. MALDI-MSI did not identify any GM3 species in the medulloblastoma xenograft, while GM3 has been reported to make up approximately 13% of total gangliosides of the human Daoy medulloblastoma cell line [4]. It is well known that cells *in situ* have different expression patterns compared to cultured cells and thus it is very likely that GM3 is not expressed in the Daoy-derived medulloblastoma *in situ*. Alternatively, the GM3 concentration was under the limit of detection of MALDI-MSI or the

irradiated area was too small. It has been shown that the amount of analyte detected by MALDI-MSI decreases as the square of the spatial resolution [44]. Normally, GM2 is a minor ganglioside in most tissues but gets highly expressed in certain cancer cells [45], including the Daoy medulloblastoma cell line [4]. We were not able to confirm the identity of the GM2 species by LC-MS/MS in the intracranial medulloblastoma xenograft because of the small amount of tissue available. However, our MALDI-MSI observation of GM2 being one of the prominent gangliosides in the intracranial medulloblastoma xenograft agrees with previous findings [4].

In conclusion, molecular imaging is a technique that permits histological investigation of molecules such as gangliosides that are involved in the structural and functional aberrations of cancer cells. Here we provide evidence that MALDI-MSI is able to discriminate between various molecular species of gangliosides expressed by different brain tumors. In the future, it might be possible to apply mass spectrometry imaging for routine clinical differentiation of brain tumors.

Supporting information

S1 Table. Principal ganglioside species identified by MALDI-MSI.
(DOCX)

S1 Fig. MALD-MSI of GM1/GD1-sialic acid and GM3 in intracranial allografts of rat glioma. MSI (A) and mass spectra (B) of GM1/GD1-sialic acid (d18:1/C18:0) and GM3 (d18:1/C24:0) in intracranial allografts of rat glioma. BF = bright field. Arrows indicate the peaks visualized in IMS. IS: Internal Standard.
(TIF)

S2 Fig. MALDI-MSI of GM1/GD1-sialic acid and GD1 in normal mouse brain. (A) MSI and mass spectra of GM1/GD1-sialic acid (d18:1/C18:0) and (B) GD1 (d18:1/C18:0) in normal mouse brain. IS: Internal Standard.
(TIF)

S3 Fig. MALDI-MSI of GM1/GD1-sialic acid in normal rat and mouse brain. The scale and intensity of ions has been changed to visualize the GM1 distribution in the white matter.
(TIF)

S4 Fig. MALD-MSI of GM3 and GM2 in intracranial allografts of rat glioma. (A) MSI of GM3 [d18:1/c24:0 - (m/z 1264)] and GM2 [d18:0/c18:0 - (m/z 1385)]. (B) Mass spectra of GM2 (d18:0/c18:0) was negative. Arrow indicate the peak of GM2 (d18:0/c18:0) visualized in IMS.
(TIF)

S5 Fig. Mass spectrometry analysis of nonpathological rat brain tissue (blue) and rat glioma allograft (red). (A) Areas cut from thick brain cryosections are marked by squares. (B) Overlay of GM1 1545 m/z from nonpathological brain tissue vs glioma allograft. (C) Overlay of GM3 1264 m/z from nonpathological brain tissue vs glioma allograft. (D) Mass spectrometric profile of GM1 and GM3 standards.
(TIF)

Author Contributions

Conceptualization: LE MP.

Funding acquisition: IC MP.

Investigation: LE EM AP BY ML.

Methodology: LE ML CCF JTR MP.

Project administration: LE IC MP.

Resources: CCF JTR.

Supervision: MP.

Validation: LE ML MP.

Visualization: LE IC MP.

Writing – original draft: LE MP.

Writing – review & editing: LE IC MP.

References

1. Hakomori S, Handa K. Glycosphingolipid-dependent cross-talk between glycosynapses interfacing tumor cells with their host cells: essential basis to define tumor malignancy. *FEBS Lett.* 2002; 531(1):88–92. PMID: [12401209](#)
2. Yu RK, Tsai YT, Ariga T, Yanagisawa M. Structures, biosynthesis, and functions of gangliosides—an overview. *J Oleo Sci.* 2011; 60(10):537–44. PubMed Central PMCID: PMC3684167. PMID: [21937853](#)
3. Fredman P, von Holst H, Collins VP, Ammar A, Dellheden B, Wahren B, et al. Potential ganglioside antigens associated with human gliomas. *Neurol Res.* 1986; 8(2):123–6. PMID: [2875407](#)
4. Chang F, Li R, Noon K, Gage D, Ladisch S. Human medulloblastoma gangliosides. *Glycobiology.* 1997; 7(4):523–30. PMID: [9184833](#)
5. Jacobsen PF, Jenkyn DJ, Papadimitriou JM. Establishment of a human medulloblastoma cell line and its heterotransplantation into nude mice. *J Neuropathol Exp Neurol.* 1985; 44(5):472–85. PMID: [2993532](#)
6. Hakomori S. Bifunctional role of glycosphingolipids. Modulators for transmembrane signaling and mediators for cellular interactions. *J Biol Chem.* 1990; 265(31):18713–6. PMID: [2229037](#)
7. Hakomori S, Igarashi Y. Gangliosides and glycosphingolipids as modulators of cell growth, adhesion, and transmembrane signaling. *Adv Lipid Res.* 1993; 25:147–62. PMID: [8396311](#)
8. Ladisch S, Li R, Olson E. Ceramide structure predicts tumor ganglioside immunosuppressive activity. *Proc Natl Acad Sci U S A.* 1994; 91(5):1974–8. PubMed Central PMCID: PMC43287. PMID: [8127917](#)
9. Ladisch S, Kitada S, Hays EF. Gangliosides shed by tumor cells enhance tumor formation in mice. *J Clin Invest.* 1987; 79(6):1879–82. PubMed Central PMCID: PMC424533. <https://doi.org/10.1172/JCI113031> PMID: [3584474](#)
10. Natoli EJ Jr., Livingston PO, Pukel CS, Lloyd KO, Wiegandt H, Szalay J, et al. A murine monoclonal antibody detecting N-acetyl- and N-glycolyl-GM2: characterization of cell surface reactivity. *Cancer Res.* 1986; 46(8):4116–20. PMID: [3731079](#)
11. Tsuchida T, Saxton RE, Morton DL, Irie RF. Gangliosides of human melanoma. *Cancer.* 1989; 63(6):1166–74. PMID: [2917320](#)
12. Wu ZL, Schwartz E, Seeger R, Ladisch S. Expression of GD2 ganglioside by untreated primary human neuroblastomas. *Cancer Res.* 1986; 46(1):440–3. PMID: [3940209](#)
13. Cornett DS, Reyzer ML, Chaurand P, Caprioli RM. MALDI imaging mass spectrometry: molecular snapshots of biochemical systems. *Nat Methods.* 2007; 4(10):828–33. <https://doi.org/10.1038/nmeth1094> PMID: [17901873](#)
14. Chan K, Lanthier P, Liu X, Sandhu JK, Stanimirovic D, Li J. MALDI mass spectrometry imaging of gangliosides in mouse brain using ionic liquid matrix. *Anal Chim Acta.* 2009; 639(1–2):57–61. <https://doi.org/10.1016/j.aca.2009.02.051> PMID: [19345758](#)
15. Dufresne M, Patterson NH, Lauzon N, Chaurand P. Assessing the Potential of Metal-Assisted Imaging Mass Spectrometry in Cancer Research. *Adv Cancer Res.* 2017; 134:67–84. <https://doi.org/10.1016/bs.acr.2016.11.003> PMID: [28110656](#)
16. Angel PM, Bayoumi AS, Hinton RB, Ru Su Y, Bichell D, Mayer JE, et al. MALDI Imaging Mass Spectrometry as a Lipidomic Approach to Heart Valve Research. *J Heart Valve Dis.* 2016; 25(2):240–52. PMID: [27989075](#)

17. Melland-Smith M, Ermini L, Chauvin S, Craig-Barnes H, Tagliaferro A, Todros T, et al. Disruption of sphingolipid metabolism augments ceramide-induced autophagy in preeclampsia. *Autophagy*. 2015; 11(4):653–69. PubMed Central PMCID: PMC4502662. <https://doi.org/10.1080/15548627.2015.1034414> PMID: 25853898
18. Shimizu Y, Satou M, Hayashi K, Nakamura Y, Fujimaki M, Horibata Y, et al. Matrix-assisted laser desorption/ionization imaging mass spectrometry reveals changes of phospholipid distribution in induced pluripotent stem cell colony differentiation. *Anal Bioanal Chem*. 2017; 409(4):1007–16. <https://doi.org/10.1007/s00216-016-0015-x> PMID: 27815610
19. Sparvero LJ, Amoscato AA, Fink AB, Anthony-muthu T, New LA, Kochanek PM, et al. Imaging mass spectrometry reveals loss of polyunsaturated cardiolipins in the cortical contusion, hippocampus, and thalamus after traumatic brain injury. *J Neurochem*. 2016; 139(4):659–75. <https://doi.org/10.1111/jnc.13840> PMID: 27591733
20. Sugiura Y, Shimma S, Konishi Y, Yamada MK, Setou M. Imaging mass spectrometry technology and application on ganglioside study; visualization of age-dependent accumulation of C20-ganglioside molecular species in the mouse hippocampus. *PLoS One*. 2008; 3(9):e3232. PubMed Central PMCID: PMC2532745. <https://doi.org/10.1371/journal.pone.0003232> PMID: 18800170
21. Zhang Y, Wang J, Liu J, Han J, Xiong S, Yong W, et al. Combination of ESI and MALDI mass spectrometry for qualitative, semi-quantitative and in situ analysis of gangliosides in brain. *Sci Rep*. 2016; 6:25289. PubMed Central PMCID: PMC485142. <https://doi.org/10.1038/srep25289> PMID: 27142336
22. Colsch B, Woods AS. Localization and imaging of sialylated glycosphingolipids in brain tissue sections by MALDI mass spectrometry. *Glycobiology*. 2010; 20(6):661–7. PubMed Central PMCID: PMC2900884. <https://doi.org/10.1093/glycob/cwq031> PMID: 20190299
23. Kettling H, Vens-Cappell S, Soltwisch J, Pirkl A, Haier J, Muthing J, et al. MALDI mass spectrometry imaging of bioactive lipids in mouse brain with a Synapt G2-S mass spectrometer operated at elevated pressure: improving the analytical sensitivity and the lateral resolution to ten micrometers. *Anal Chem*. 2014; 86(15):7798–805. <https://doi.org/10.1021/ac5017248> PMID: 25007005
24. Whitehead SN, Chan KH, Gangaraju S, Slinn J, Li J, Hou ST. Imaging mass spectrometry detection of gangliosides species in the mouse brain following transient focal cerebral ischemia and long-term recovery. *PLoS One*. 2011; 6(6):e20808. PubMed Central PMCID: PMC3110773. <https://doi.org/10.1371/journal.pone.0020808> PMID: 21687673
25. Woods AS, Colsch B, Jackson SN, Post J, Baldwin K, Roux A, et al. Gangliosides and ceramides change in a mouse model of blast induced traumatic brain injury. *ACS Chem Neurosci*. 2013; 4(4):594–600. PubMed Central PMCID: PMC3629744. <https://doi.org/10.1021/cn300216h> PMID: 23590251
26. Schmidek HH, Nielsen SL, Schiller AL, Messer J. Morphological studies of rat brain tumors induced by N-nitrosomethylurea. *J Neurosurg*. 1971; 34(3):335–40. <https://doi.org/10.3171/jns.1971.34.3.0335> PMID: 5547317
27. Chen CT, Kitson AP, Hopperton KE, Domenichiello AF, Trepanier MO, Lin LE, et al. Plasma non-esterified docosahexaenoic acid is the major pool supplying the brain. *Sci Rep*. 2015; 5:15791. PubMed Central PMCID: PMC4625162. <https://doi.org/10.1038/srep15791> PMID: 26511533
28. Zou J, Talbot F, Tata A, Ermini L, Franjic K, Ventura M, et al. Ambient Mass Spectrometry Imaging with Picosecond Infrared Laser Ablation Electrospray Ionization (PIR-LAESI). *Anal Chem*. 2015; 87(24):12071–9. <https://doi.org/10.1021/acs.analchem.5b02756> PMID: 26561279
29. Joza S, Wang J, Tseu I, Ackerley C, Post M. Fetal, but not postnatal, deletion of semaphorin-neuropilin-1 signaling affects murine alveolar development. *Am J Respir Cell Mol Biol*. 2013; 49(4):627–36. <https://doi.org/10.1165/rcmb.2012-0407OC> PMID: 23713442
30. Rodighiero C, Fujinaga Y, Hirst TR, Lencer WI. A cholera toxin B-subunit variant that binds ganglioside G(M1) but fails to induce toxicity. *J Biol Chem*. 2001; 276(40):36939–45. <https://doi.org/10.1074/jbc.M104245200> PMID: 11479294
31. Chen L, Miao W, Tang X, Zhang H, Wang S, Luo F, et al. The expression and significance of neuropilin-1 (NRP-1) on glioma cell lines and glioma tissues. *J Biomed Nanotechnol*. 2013; 9(4):559–63. PMID: 23621014
32. Snuderl M, Batista A, Kirkpatrick ND, Ruiz de Almodovar C, Riedemann L, Walsh EC, et al. Targeting placental growth factor/neuropilin 1 pathway inhibits growth and spread of medulloblastoma. *Cell*. 2013; 152(5):1065–76. PubMed Central PMCID: PMC3587980. <https://doi.org/10.1016/j.cell.2013.01.036> PMID: 23452854
33. Seyfried TN, Mukherjee P. Ganglioside GM3 Is Antiangiogenic in Malignant Brain Cancer. *J Oncol*. 2010; 2010:961243. PubMed Central PMCID: PMC2904445. <https://doi.org/10.1155/2010/961243> PMID: 20634908

34. Wikstrand CJ, Fredman P, McLendon RR, Svennerholm L, Bigner DD. Altered expression of ganglioside phenotypes of human gliomas in vivo and in vitro. *Mol Chem Neuropathol*. 1994; 21(2–3):129–38. <https://doi.org/10.1007/BF02815347> PMID: 7522005
35. van Echten-Deckert G, Gurgui M. Golgi localization of glycosyltransferases involved in ganglioside biosynthesis. *Curr Drug Targets*. 2008; 9(4):282–91. PMID: 18393822
36. Heffer-Lauc M, Cacic M, Judas M, Muthing J. Anti-GM3 (II3Neu5Ac-lactosylceramide) ganglioside antibody labels human fetal Purkinje neurons during the critical stage of cerebellar development. *Neurosci Lett*. 1996; 213(2):91–4. PMID: 8858616
37. Hanai N, Nakamura K, Shitara K. Recombinant antibodies against ganglioside expressed on tumor cells. *Cancer Chemother Pharmacol*. 2000; 46 Suppl:S13–7. PMID: 10950141
38. Tringali C, Lupo B, Cirillo F, Papini N, Anastasia L, Lamorte G, et al. Silencing of membrane-associated sialidase Neu3 diminishes apoptosis resistance and triggers megakaryocytic differentiation of chronic myeloid leukemic cells K562 through the increase of ganglioside GM3. *Cell Death Differ*. 2009; 16(1):164–74. <https://doi.org/10.1038/cdd.2008.141> PMID: 18820643
39. Watanabe R, Ohyama C, Aoki H, Takahashi T, Satoh M, Saito S, et al. Ganglioside G(M3) overexpression induces apoptosis and reduces malignant potential in murine bladder cancer. *Cancer Res*. 2002; 62(13):3850–4. PMID: 12097299
40. Kiura K, Watarai S, Ueoka H, Tabata M, Gemba K, Aoe K, et al. An alteration of ganglioside composition in cisplatin-resistant lung cancer cell line. *Anticancer Res*. 1998; 18(4C):2957–60. PMID: 9713491
41. Uemura S, Kabayama K, Noguchi M, Igarashi Y, Inokuchi J. Sialylation and sulfation of lactosylceramide distinctly regulate anchorage-independent growth, apoptosis, and gene expression in 3LL Lewis lung carcinoma cells. *Glycobiology*. 2003; 13(3):207–16. <https://doi.org/10.1093/glycob/cwg022> PMID: 12626418
42. Giussani P, Tringali C, Riboni L, Viani P, Venerando B. Sphingolipids: key regulators of apoptosis and pivotal players in cancer drug resistance. *Int J Mol Sci*. 2014; 15(3):4356–92. PubMed Central PMCID: PMC3975402. <https://doi.org/10.3390/ijms15034356> PMID: 24625663
43. Zamfir AD. Neurological analyses: focus on gangliosides and mass spectrometry. *Adv Exp Med Biol*. 2014; 806:153–204. https://doi.org/10.1007/978-3-319-06068-2_8 PMID: 24952183
44. Boggio KJ, Obasuyi E, Sugino K, Nelson SB, Agar NY, Agar JN. Recent advances in single-cell MALDI mass spectrometry imaging and potential clinical impact. *Expert Rev Proteomics*. 2011; 8(5):591–604. PubMed Central PMCID: PMC3268336. <https://doi.org/10.1586/epr.11.53> PMID: 21999830
45. Hamilton WB, Helling F, Lloyd KO, Livingston PO. Ganglioside expression on human malignant melanoma assessed by quantitative immune thin-layer chromatography. *Int J Cancer*. 1993; 53(4):566–73. PMID: 8436430